Critical Dynamics near the Oscillatory Instability in Rayleigh-Bénard Convection

R. E. Ecke, Y. Maeno, H. Haucke, and J. C. Wheatley
Los Alamos National Laboratory, Los Alamos, New Mexico 87545
(Received 6 August 1984)

The oscillatory temperature amplitude of a low–Prandtl-number fluid in Rayleigh-Bénard convection is shown to exhibit critical slowing down near the onset of oscillatory convection. The data are analyzed in the context of a mean-field Landau-Hopf equation. We find the magnitude of the power-law exponent for the dynamic relaxation to be 1.01 ± 0.02 and 1.00 ± 0.02 above and below onset, respectively, in agreement with the theoretical predictions.

PACS numbers: 67.60.–g, 44.25.+f, 47.20.+m

We have studied Rayleigh-Bénard convection in a ^{3}He–superfluid-^{4}He solution with ^{3}He atomic concentration of 1.46%. In a large temperature range, these dilute solutions have been shown[1-3] to exhibit effectively single-component properties with very low Prandtl number; the present solution at 0.85 K has a Prandtl number of 0.066. In this system, the first two convective instabilities that are observed as the Rayleigh number is increased are the onset of classical Rayleigh time-independent (stationary) convection and the onset of time-dependent (oscillatory) convection. This paper investigates the steady state and dynamic properties of the latter instability.

Instabilities in many systems far from equilibrium exhibit features of equilibrium phase transitions.[4] The exact nature of this correspondence is of great interest.[5,6] The Rayleigh-Bénard convective instabilities should provide excellent examples of this analogy. In particular, they should serve as classic illustrations of mean-field phase transitions because hydrodynamic fluctuations are small except extremely close to onset.[7] Indeed, both Behringer and Ahlers[8] and Weisfreid *et al.*[9] can describe the dynamic and steady-state properties of the stationary convective instability using a Landau-Hopf formalism.

In contrast, for the oscillatory convective instability, although Libchaber and Maurer[10] have observed critical slowing down of the oscillatory temperature amplitude below onset, there have been no reported measurements above onset or detailed comparison with Landau-Hopf theory. We have measured both the steady-state and transient properties of the oscillatory temperature amplitude both above and below onset and found this transition to be a classic example of the Landau-Hopf formalism.

The experimental system in which we study Rayleigh-Bénard convection has been described in detail elsewhere.[1,2] In addition to aspect ratio, the two dimensionless parameters that characterize single-component convection are the Rayleigh (R) and Prandlt (σ) numbers defined as

$$R \equiv g\beta d^3 \Delta T/\nu\kappa \quad \text{and} \quad \sigma = \nu/\kappa, \tag{1}$$

where g is the acceleration of gravity, β is the thermal expansion coefficient, d is the cell height, ΔT is the top-bottom temperature difference, ν is the kinematic viscosity, and κ is the thermal diffusivity. We also define the stress parameter for stationary convection as $\epsilon \equiv R/R_c - 1$, where R_c is the Rayleigh number at the onset of stationary convection. The temperature of the bottom plate of the cell for the present work is 0.85 K, for which the measured R_c is 2033, the calculated Prandtl number is 0.066, and R at the onset of oscillations is about 1.1×10^4. Our cell is rectangular with aspect ratios $\Gamma = L/2d = 1.0$ and $\Gamma' = W/2d = 0.70$, where L and W are the length and width of the sides, respectively, and $d = 0.80$ cm is the cell height.

Another characteristic of our experimental cell is a highly sensitive local temperature probe (a differential SQUID thermocouple) which measures the horizontal temperature difference between a small, weakly thermally isolated center plug and the rest of the top plate. Another similar thermocouple measures the top-bottom temperature difference. The high sensitivity of these thermometers,[11] the actual physical design of the cell, particular aspects of the measurement technique,[2,12] and special properties of the solutions[1-3] are described elsewhere.

Below ϵ_0, the value of the stress parameter at the onset of oscillatory convection, the convective flow is stationary and thought to have the form of two parallel rolls with fluid rising in the center. As reported previously,[2] above ϵ_0 the rms oscillatory temperature amplitude increases continuously with a linear dependence on ϵ from zero amplitude at ϵ_0. The oscillations have a single frequency which varies as $\epsilon^{1/2}$. When the heat flow into the top plate is suddenly increased or decreased, a nonsteady state is created. The observed return to a steady-state configuration occurs through relaxation of both the nonoscillatory and the oscillatory com-

ponents of the temperature field. The vertical thermal diffusion time is $\tau_\kappa \equiv 4d^2/\pi^2\kappa = 3.56$ s at 0.96 K (the mean cell temperature at ϵ_0), and the relaxation time of the nonoscillatory temperature field is τ_c. τ_c is obtained from an exponential fit to the relaxation of the dc component of either the probe or the top-bottom thermocouple. For $0.4 > \xi > -0.4$, where $\xi \equiv \epsilon - \epsilon_0$, we find τ_c/τ_κ to be constant within experimental error with an average value of 0.64. Experimentally we find that the characteristic time τ associated with changes of the oscillatory amplitude is much longer than τ_c in the range noted above. We separate the influence of τ_c from the determination of τ in the analysis by waiting $4\tau_c$ before fitting the decay envelope for τ. As a physical consequence, the thermal properties of the fluid during the analyzed decay are characteristic of the final state ξ.

The measurement of the relaxation time of the oscillatory envelope for $\xi > 0$ included increasing the heat flow by a small increment or decreasing it by the same increment to achieve the same final state ξ. For final states $\xi < 0$, the heat flow was suddenly decreased to the final state from an initial state, chosen conveniently as $\xi = 0.2$, above the onset. Figures 1(a) and 1(c) show examples of the relaxation of the oscillations for final-state values above and below onset, respectively. Note that for $\xi < 0$, the oscillation amplitude does not decay strictly to zero but is limited by the background noise whose magnitude is about 0.3 μK. This introduces a complication in the analysis which we discuss below.

Both the steady-state properties and the dynamic relaxation of the oscillatory amplitude can be represented by a Landau-Hopf equation which McLaughlin and Martin[13] showed can be obtained in an approximation to the Boussinesq equations. The dynamic equation for the order parameter A (proportional to the magnitude of the oscillatory convective velocity) contains terms linear and cubic in A. However, the quantity which we measure, the envelope amplitude E, is related to the horizontal temperature gradient over a cross section of the cell, which, following Ref. 13, varies as the square of the order parameter. Thus one finds for the time rate of change of the oscillatory envelope

$$dE/dt = c_1 \xi E - c_3 E^2. \quad (2)$$

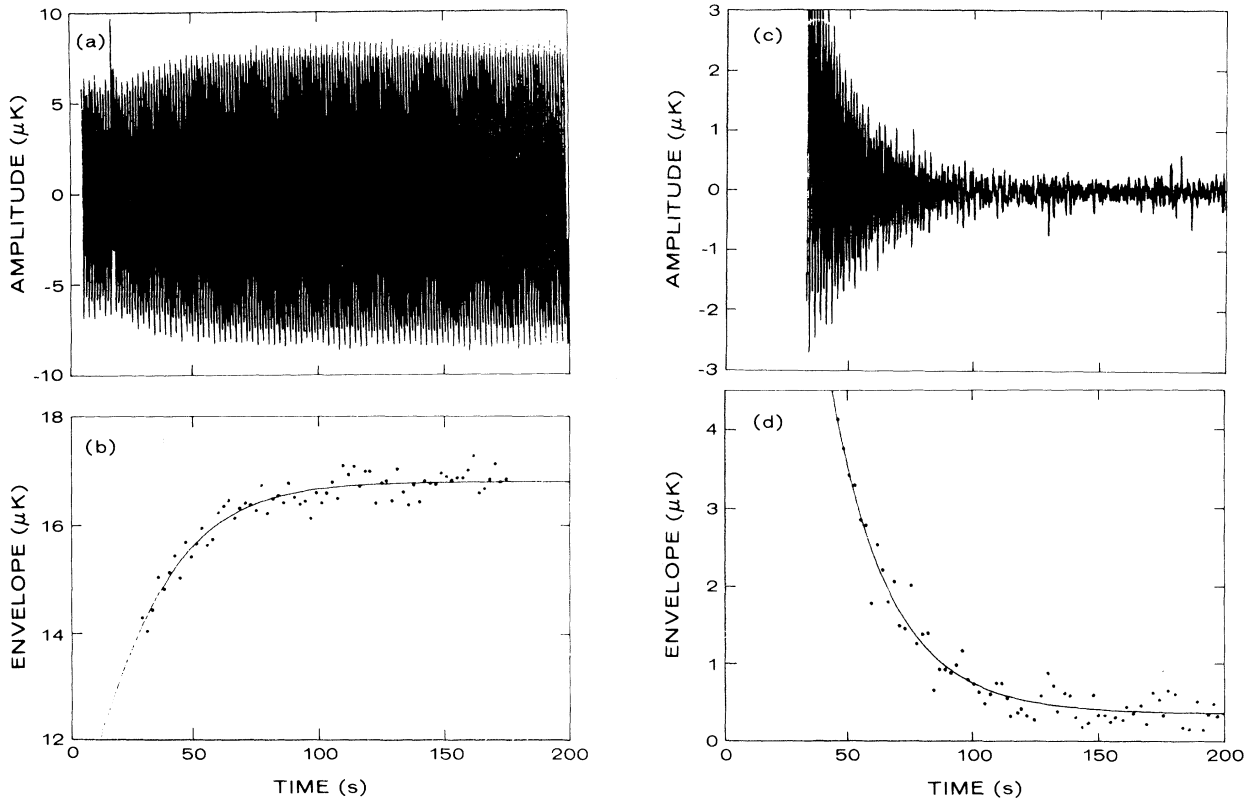

FIG. 1. Time series and resultant analysis of the envelope amplitude vs time for (a),(b) $\xi = +0.219$ and (c),(d) $\xi = -0.193$. The sharp spike in (a) is due to the abrupt change of the heat flow from the initial to final state.

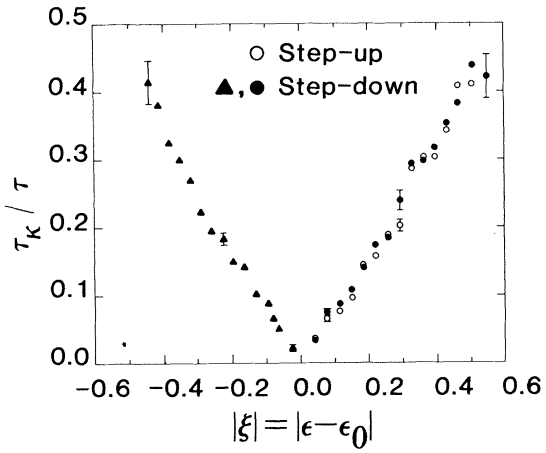

FIG. 2. Inverse of characteristic time τ of the oscillatory envelope normalized by τ_κ plotted as a function of the final state ξ. The error bars represent the variance in the characteristic time due to the fitting procedure.

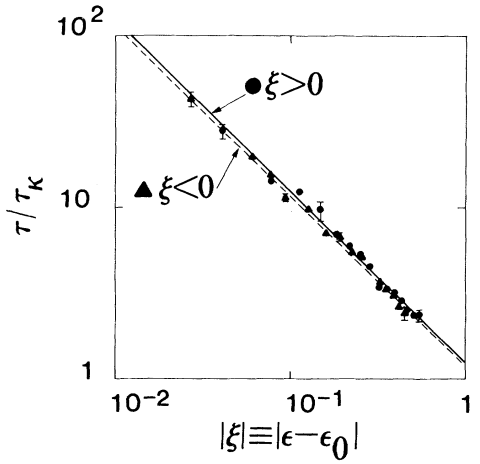

FIG. 3. Characteristic time τ of the oscillatory envelope normalized by τ_κ vs $|\xi| \equiv |\epsilon - \epsilon_0|$ plotted on a full logarithmic scale. The error bars are as in Fig. 2 and for $\xi > 0$ the average values of step-up and step-down measurements are used. The solid and dashed lines are least-squares fits as described in the text for $\xi > 0$ and $\xi < 0$, respectively.

The steady-state solutions obtained by setting $dE/dt = 0$ are $E_- = 0$ and $E_+ = c_1\xi/c_3$, corresponding to solutions below and above onset, respectively. This ξ dependence of the steady-state amplitude is in excellent agreement with our observations. By integrating (2), one obtains for ξ above and below onset the time-dependent solution

$$E(t) = \left[\frac{c_3}{c_1\xi} + \left(\frac{1}{E(t=0)} - \frac{c_3}{c_1\xi}\right)e^{-2c_1\xi}\right]^{-1} \quad (3)$$

from which one defines the characteristic time $\tau = 1/(c_1|\xi|) \equiv \tau_0|\xi|^{-1}$. We have fitted the envelope data above the onset with Eq. (3), see Fig. 1(b), and have found good agreement between values of τ for step-up and step-down jumps to the same final value of ξ. In contrast, a simple exponential fit of the asymptotic form of Eq. (3) yields different values of τ for the different jumps; the step-up time constants are systematically larger than the step-down values. The differences range from 15% at $\xi = 0.45$ to 50% at $\xi = 0.05$ while we estimate that the error due to the fit in τ is less than 10%. This fact from the analysis gives substantial support to the validity of the full form of Eq. (2) for the time dependence of E.

As a check on the consistency of the fitting procedure we have analyzed the fitted final value of E obtained in the dynamic measurements to check its linear dependence on ϵ. We find that the linearity of E is very good with very small scatter of the individual points from the line. A least-squares fit gives $\epsilon_0 = 4.172 \pm 0.02$ compared to 4.178 ± 0.01 for ϵ_0 measured independently from rms amplitude data.

For step-down data when the final state is below the onset, the envelope decays to a small value limited by the background noise; see Fig. 1(d). This nonzero value complicates the fitting procedure because at large amplitudes the noise adds with random phase and merely increases the scatter of E, whereas at near-zero amplitude the noise is the entire envelope. Because of the small amplitudes involved, a fit by Eq. (3) is poorly behaved. Special care was taken to use data at long times only, so that one could use the asymptotic form of Eq. (3); a simple exponential with an added constant term to represent the noise [see Fig. 1(d)]. Corrections due to the nonadditivity of the noise and to the use of the asymptotic form of the Landau equation tend to cancel according to a computer simulation, and we estimate that the error in τ due to the use of the asymptotic form of (3) plus a constant noise term is less than 10%.

The resultant characteristic times determined from the analysis discussed above are plotted in the dimensionless form of τ_κ/τ vs ξ, linearly in Fig. 2 and on a log-log scale in Fig. 3. It is essential to note that $\xi = \epsilon - \epsilon_0$ is evaluated from the final value of ϵ after a step-up or step-down and from ϵ_0 independently determined from the steady-state data. The data in Fig. 3 show an excellent fit with the equation

$$\tau = \tau_0|\xi|^{-\nu}. \quad (4)$$

A least-squares fit to the data yields

$$\tau_0 = (1.24 \pm 0.04)\tau_\kappa, \quad y = 1.01 \pm 0.02$$

for $\xi > 0$, and

$$\tau_0 = (1.19 \pm 0.03)\tau_\kappa, \quad y = 1.00 \pm 0.02$$

for $\xi < 0$, in agreement with classical predictions for the exponent.[14] For the prefactor, there is sharp disagreement with theoretical predictions,[13] calculated for the case of free top-bottom boundaries and $\Gamma = \infty$. However, the small aspect ratio and rigid boundaries appropriate for our experimental conditions are probably important factors in determining τ_0.

A detailed description of this work is in preparation.

[1]P. Warkentin, H. Haucke, P. Lucas, and J. Wheatley, Proc. Nat. Acad. Sci. U.S.A. **77**, 6983 (1980).

[2]Y. Maeno, H. Haucke, and J. Wheatley, to be published.

[3]A. Fetter, Phys. Rev. B **26**, 1164, 1174 (1982).

[4]See, for example, C. Normand, Yves Pomeau, and M. Velarde, Rev. Mod. Phys. **49**, 581 (1977).

[5]P. W. Anderson, in *Basic Notions of Condensed Matter Physics* (Benjamin/Cummings, Menlo Park, California, 1984).

[6]L. Sneddon, Phys. Rev. A **24**, 1629 (1981).

[7]R. Graham, Phys. Rev. A **10**, 1762 (1974).

[8]J. Weisfreid, Y. Pomeau, M. Dubois, C. Normand, and P. Bergé, J. Phys. Lett. (Paris) **39**, L725 (1978).

[9]R. Behringer and G. Ahlers, Phys. Lett. **62A**, 329 (1977).

[10]A. Libchaber and J. Maurer, in *Proceedings of the NATO Advanced Study Institute on Nuclear Phenomena at Transitions and Instabilities,* edited by T. Riste (Plenum, New York, 1981).

[11]Y. Maeno, H. Haucke, and J. Wheatley, Rev. Sci. Instrum. **54**, 946 (1983).

[12]Y. Maeno, H. Haucke, R. Ecke, and J. Wheatley, to be published.

[13]J. McLaughlin and P. Martin, Phys. Rev. **A12**, 186 (1975).

[14]In general critical-dynamics notation, the reduced temperature exponent of the characteristic relaxation time is $z\nu$, where the classical values of z and ν are 2 and $\frac{1}{2}$, respectively.